Measurements of Radial Profiles of He^{2+} Transport Coefficients on the TFTR Tokamak

E. J. Synakowski, B. C. Stratton, P. C. Efthimion, R. J. Fonck,[a] R. A. Hulse, D. W. Johnson, D. K. Mansfield, H. Park, S. D. Scott, and G. Taylor

Princeton Plasma Physics Laboratory, Princeton University, Princeton, New Jersey 08543

(Received 16 May 1990)

Measurements of the spatial structure of the transport coefficients of He^{2+} on the Tokamak Fusion Test Reactor is reported. He^{2+} profiles were measured using charge-exchange spectroscopy after a helium puff into corotating L-mode plasmas. Modeling shows that the He^{2+} diffusivity is about 10 m^2/s near the plasma edge and drops to below 1 m^2/s inside of the $q=1$ surface. The convective velocity ranges from 1–3 m/s near $q=1$ to 20–40 m/s near the edge. The helium diffusivity is on the order of the ion momentum and thermal diffusivity and is greater than the electron thermal diffusivity.

PACS numbers: 52.25.Fi, 52.25.Vy, 52.55.Fa

The behavior of helium ash in a tokamak plasma will be of tremendous importance to the cost and operations of future fusion devices. The details of the relationship between thermal helium particle transport and energy transport will be a determining factor of helium pumping and plasma current requirements, and may determine whether a fusion burn can in fact be sustained.[1-3] Detailed knowledge of both helium particle and heat transport coefficients is required to confidently predict the performance of future fusion devices. Knowledge of local transport coefficients allows a more powerful basis for prediction than does scaling of observed confinement times from present devices, as such measurements always contain ambiguities due to source effects, differences in gradients between experiments, etc. Characterization of the transport of ionic plasma species also serves as powerful leverage when comparing experiment to various transport theories, encouraging the possibility of using theory-based modeling as a reliable predictor of future tokamak performance. Previous measurements of helium transport are scarce, and those available have been spatially averaged.[4,5] In this Letter we describe the first measurements of the spatial structure of transport coefficients of He^{2+} in a tokamak plasma, and demonstrate that the techniques used enable detailed comparisons between particle, heat, and momentum transport. Charge-exchange recombination spectroscopy[6] (CHERS) has been used to measure the time evolutions of the density of $He^{2+}(r)$ at several radial locations following a helium puff on the Tokamak Fusion Test Reactor (TFTR). The temporal behavior of the He^{2+} density has been modeled with the impurity transport code MIST,[7] allowing the spatial structure of transport coefficients to be deduced. The transport coefficients have indeed been found to have large spatial variations, increasing by a factor of several between the sawtooth inversion radius and the plasma edge. Diffusivities and convective velocities in this region are at least an order of magnitude above those predicted by neoclassical theory.[8,9] Inside the inversion radius, transport rates are reduced, but are still larger than neoclassical values except possibly near the magnetic axis.

The plasmas for this experiment had a major radius of 2.45 m, a minor radius of 0.80 m, a plasma current of 1.4 MA, a toroidal field of 4 T, and a discharge duration of 6 s. These deuterium plasmas were heated with 7 MW of codirected tangential deuterium neutral beam injection from 3.5 to 4.5 s. The average electron density during the density flattop was 2.5×10^{19} m^{-3}/s. The electron-density peaking parameter, the ratio of the central density to the average density $n_e(0)/\langle n_e\rangle$, was 1.6, typical of most low-density L-mode discharges on TFTR, while the energy confinement time τ_E was modestly higher than the L-mode value ($\tau_E=1.3\tau_{E_{L\text{-mode}}}$). The central ion temperature was 9–10 keV during the beam flattop, and the central electron temperature was ~5 keV. The central toroidal velocity was ~250 km/s, and the central Z_{eff} was 4.0. These discharges possessed sawteeth with ~150–200 ms duration and had an inversion radius at $r/a=0.35$, where r is the plasma minor radius and a is the limiter radius. A 16-ms helium puff was introduced at 4.2 s, well into the equilibrium phase of the neutral beam pulse. The line-averaged density of the plasma increased by (2–3)% as a result of the puff; the electron temperature decreased $<2\%$.

The CHERS spectrometer was used to view a coinjecting heating beam. The neutral-beam–CHERS sightline intersection radii are separated by ~0.1 m. The He^{2+} density evolution after the puff was measured by following the time behavior of the 4686-Å line ($n=4$–3) of He^{1+}, induced by charge-exchange recombination with beam neutrals. Time resolution for these measurements was 10 ms, and the data from fourteen discharges were averaged together without regard to sawtooth phase. Interpretation of measured line brightnesses can be complicated by the presence of He^{1+} ions (ion plume) produced by charge exchange and subsequently excited by electron impact.[6] For tangential views through the center of the plasma, the plume brightnesses can rival the prompt charge-exchange signal and must therefore be taken into account. He^{2+} profiles were deduced using a self-consistent treatment in which trial He^{2+} profile

© 1990 The American Physical Society

shapes were iterated until agreement between predicted and observed line brightnesses was achieved. Beam attenuation was calculated using the mean-free-path treatment of Boley, Janev, and Post[10] and reaction-rate coefficients for inducing the $n=4$–3 transition were taken from measurements by Ciric *et al.*[11] The reaction-rate coefficient for exciting this transition by charge exchange from the $n=2$ level of beam neutrals,[12] important for the one-third ($E/3$) energy component of the beam, has been calculated using the classical trajectory Monte Carlo (CTMC) code of Olson and Salop.[13] Where the $E/3$ component is not significantly attenuated, this increases the total line emission reaction rate by at most 15%. This effect has been included in these measurements. With central ion temperatures of ~ 10 keV, charge exchange from thermal halos is negligible.[14]

The time evolution of the densities was modeled by solving the one-dimensional continuity equations for the helium ions:

$$\partial/\partial t(n_q)+(1/r)\partial/\partial r(r\Gamma_q)=-(I_q+R_q)n_q+I_{q-1}n_{q-1}+R_{q+1}n_{q+1}-n_q/\tau_{\parallel}+S_q\,, \quad (1)$$

where q is the ion charge, n_q is the density of charge state q, Γ_q is the radial flux for charge state q, R_q is the recombination rate, I_q is the ionization rate, $\tau_{\parallel}$ is an effective loss rate for particles outside the limiter radius, and S_q is a volume source for $q=+1$ ions due to edge neutral influx. It is assumed that the helium flux can be expressed as

$$\Gamma_q(r,t)=-D_{\mathrm{He}}(r)\partial/\partial r(n_q(r,t))+V_{\mathrm{He}}(r)n_q(r,t)\,, \quad (2)$$

where D_{He} is the helium diffusivity and V_{He} is the convective velocity. Transport of He^{1+} and He^{2+} are assumed to be the same. The neutral helium source has been programmed into MIST by assuming that the energy of recycled neutral helium is 0.1 eV, typical of the temperature of a carbon tile on the bumper limiter. The use of energies lower than this does not affect the transport conclusions presented here; energies on the order of an eV or more are unphysical and give time histories of edge densities that cannot be modeled with any values of D_{He} and V_{He}. The time behavior of the He^{2+} source was deduced from measurements of the 304-Å He^{1+} line ($n=2$–1) by a vacuum-ultraviolet spectrometer viewing along a radial chord at the inner wall limiter, the location of most of the recycling. Use of this measurement of the source eliminates the need for any assumptions regarding helium recycling efficiency.

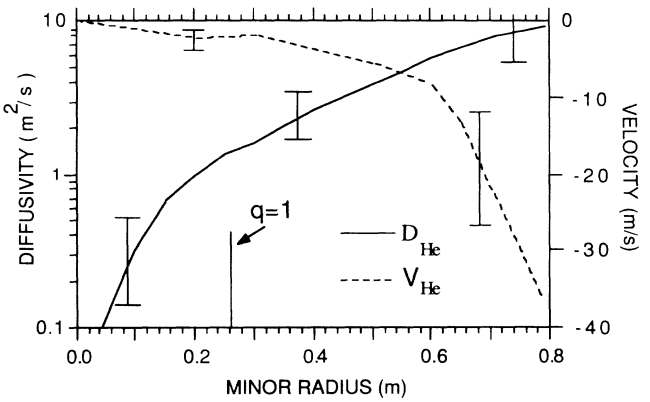

FIG. 1. Diffusivity and convective velocity of He^{2+} as functions of radius. Error bars indicate estimated range of acceptable transport coefficients, including statistical errors and those due to uncertainties in He^{2+} profile shape.

In the modeling, D_{He} and V_{He} are constrained to reproduce the He^{2+} profile observed long after the puff (>250 ms). Under this constraint, it is found that no spatially constant D_{He} will reproduce the data satisfactorily. The ranges of D_{He} and V_{He} that best fit the data are shown in Fig. 1. Here, D_{He} was allowed to vary linearly between the radii at which helium densities were measured. Errors in the inferred transport coefficients were established by including estimates of the uncertainty of the best fits as well as propagating a $\pm 20\%$ uncertainty in the beam stopping cross sections through the profile-shape calculations. Less satisfactory fits were obtained near the plasma axis, possibly because sawtoothing effects were not completely averaged out in this ensemble of data. Still, examination of predicted profile shapes indicates that the best-fit D_{He} increases rapidly

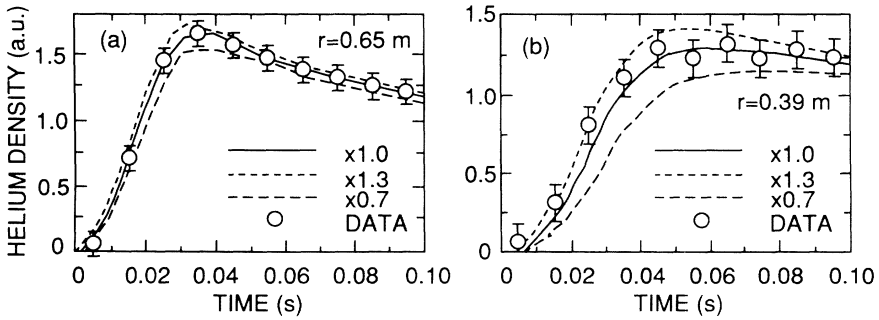

FIG. 2. Measured He^{2+} density and MIST modeling results for the transport coefficients in Fig. 1 (hollow D_{He}) $\pm$ 30% variations in the diffusivity (with $D_{\mathrm{He}}/V_{\mathrm{He}}$ constrained as discussed in the text).

with minor radius inside the $q=1$ surface. Of note is that the good-fit $D_{He}(r)$ varies by over an order of magnitude across the plasma, with the extreme values found near the plasma boundary and inside the inversion radius. Figure 2 shows the measured local He^{2+} density at (a) $r=0.65$ and (b) $r=0.39$ m. Error bars represent estimates of the statistical uncertainty in the measured signal brightnesses. Also shown in this figure are MIST modeling results using $D_{He}(r)$ and $V_{He}(r)$ of Fig. 1 and results from varying this form of $D_{He}(r)$ by $\pm 30\%$ (again with D_{He}/V_{He} chosen to reproduce the long-time He^{2+} profile). Even modest variations in the assumed diffusivity predict transport times that are outside of the statistical errors.

Measured and modeled profiles after the puff are shown in Fig. 3. Figure 3(a) shows the profiles inferred from CHERS measurements. Note the short time scales (~ 50 ms) required for the profile at $r/a > 0.5$ to reach its final scale length. However, the time scale required to reach the final scale length for $r/a < 0.5$ is typically ~ 100 ms, indicative of slower transport there. Figure 3(b) shows the modeled profile shapes from MIST using the transport coefficients of Fig. 1. Good reproduction of the measured profiles is achieved. However, the profiles obtained using the constant D_{He} required to match the data near the plasma edge do not reproduce the measured time evolutions [Fig. 3(c)]; transport is predicted to be much too rapid in the interior. A more modest value of constant D_{He}, typical of the value near $r/a=0.5$ from Fig. 1, also fails to reproduce the profile evolutions observed [Fig. 3(d)].

Thermal and momentum transport coefficients have been calculated using the 1D steady-state transport code SNAP. Figure 4 shows D_{He}, the ion thermal diffusivity χ_i, the ion momentum diffusivity χ_ϕ, and the electron thermal diffusivity χ_e. Error estimates of χ_i, χ_ϕ, and χ_e were obtained by performing 100 transport analyses using the measured profiles (n_e as measured by a ten-channel infrared interferometer, T_e as measured by electron cyclotron emission, and T_i and V_ϕ as measured by CHERS) and other input data simultaneously varied within their ranges of uncertainty by Monte Carlo sampling a Gaussian distribution for both statistical and systematic errors.[15] Profiles were obtained near the top of a sawtooth cycle. Interestingly, it is found that $D_{He}(r) \sim \chi_i(r) \sim \chi_\phi(r) > \chi_e(r)$ over much of the plasma cross section (Fig. 4). If electrostatic turbulence is the dominant transport mechanism, this relation between $D_{He}(r)$ and $\chi_i(r)$ is to be expected. If helium can be regarded as a trace impurity, its transport is not tied to the constraints of ambipolarity. The helium ions can then be expected to transport at a rate comparable to the ion thermal energy, consistent with $D_{He}(r) \sim \chi_i(r)$. In contrast, these results are in sharp disagreement with magnetic turbulence models, which predict that $D_{He}/\chi_e \sim (m_e/m_{He})^{1/2}$. This work is being carried out in conjunction with iron transport measurements using CHERS.[16] Indications are that the heliumlike iron diffusion coefficient is comparatively flat and the convective velocity is considerably smaller than that found for He^{2+}. Further examination of the details of the predicted ratios of the helium, iron, and heat fluxes may yield useful constraints on the scale size of turbulence and information on rotation effects. Results from such a study will be described in a more comprehensive publication.

In this context, it has been pointed out that depen-

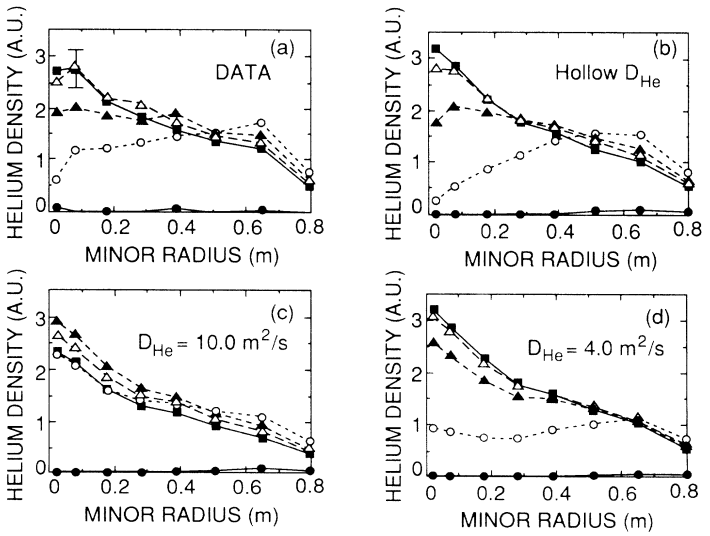

FIG. 3. Helium profiles for various times after the puff. (a) Measured. (b) Simulated with MIST with D_{He} and V_{He} from Fig. 1. (c) From MIST, with $D_{He}=10$ m^2/s. (d) From MIST, with $D_{He}=4$ m^2/s. In (b)-(d), D_{He}/V_{He} is constrained to reproduce the long-time (>120 ms) scale length. Solid circles, $t=0.005$ s after puff; open circles, $t=0.035$ s; solid triangles, $t=0.065$ s; open triangles, $t=0.095$ s; closed squares, $t=0.125$ s.

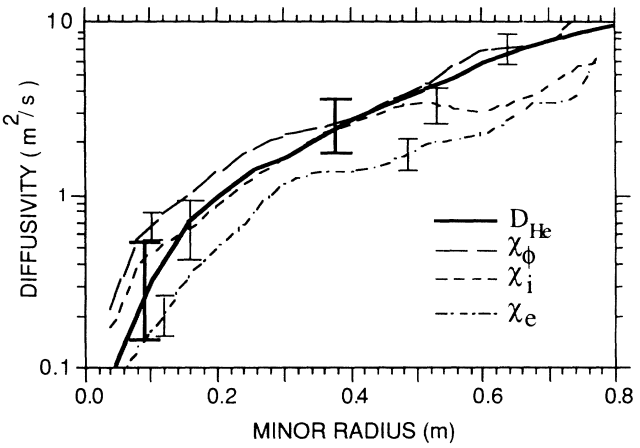

FIG. 4. Helium diffusivity $D_{He}(r)$ with electron thermal diffusivity χ_e, ion thermal diffusivity χ_i, and ion momentum diffusivity χ_ϕ as calculated with SNAP.

dences of the transport coefficients on plasma parameters can cause the perturbative phase of the transport to deviate significantly from that in steady state if the transport coefficients are functions of bulk plasma quantities such as n_e, ∇n_e, T_e, ∇T_e, etc.[17] Such dependences are predicted by drift-wave theories.[18] In the case of electron-transport experiments with gas puffing, this is especially important because the fractional change in n_e and ∇n_e as a result of the perturbation may be the same order as the fractional change in the transport coefficients themselves. However, the problem is of greatly reduced order for impurity transport experiments involving gas puffing or impurity injection. If the fluctuations assumed to be driving impurity transport are not changed significantly by the introduction of the impurity itself, then the fractional change in n_{He} and ∇n_{He} can easily be an order of magnitude larger than the fractional change in the transport coefficients (again determined by bulk plasma parameters). In this experiment, the fraction of ions n_i/n_e is less than 2% for helium, far below that of the thermal deuterons (~30%), slowing-down beam ions (~15%), and carbon (~8%), making it unlikely that a large change in helium transport coefficients results from the introduction of helium itself. Of course, this issue deserves examination by introducing various size gas puffs and will be the subject of future experiments.

The authors gratefully acknowledge fruitful conversations with S. Cowley. The generosity and support of R. E. Olson for making his CTMC code available is greatly appreciated. It is a pleasure to acknowledge the support of the TFTR physicists, engineers, and computer operators. This research was conducted under DOE Grant No. DE-AC02-76-CHO-3703.

[a]Permanent address: Department of Nuclear Engineering and Engineering Physics, University of Wisconsin at Madison, Madison, WI 53706.

[1]F. Engelmann and A. Nocentine, Comments Plasma Phys. Controlled Fusion **5**, 253 (1980).

[2]R. J. Taylor, B. D. Fried, and G. J. Morales, Comments Plasma Phys. Controlled Fusion **13**, 227 (1990).

[3]M. H. Redi and S. A. Cohen, Princeton Plasma Physics Laboratory Report No. PPPL-2641, 1990 (to be published).

[4]J. D. Strachan *et al.*, Nucl. Fusion **22**, 1145 (1982).

[5]R. J. Fonck and R. A. Hulse, Phys. Rev. Lett. **47**, 796 (1981).

[6]R. J. Fonck, D. S. Darrow, and K. P. Jaehnig, Phys. Rev. A **29**, 3288 (1984).

[7]R. A. Hulse, Nucl. Technol. Fusion **3**, 259 (1983).

[8]P. H. Rutherford *et al.*, in *Proceedings of the International Symposium on Plasma Wall Interactions, Julich, Federal Republic of Germany* (Pergamon Press for the Commission of European Communities, Oxford, 1977).

[9]S. P. Hirshman, Phys. Fluids **21**, 224 (1978).

[10]C. D. Boley, R. K. Janev, and D. E. Post, Phys. Rev. Lett. **52**, 534 (1984).

[11]D. Ciric, R. Hoekstra, F. J. de Heer, and R. Morgenstern, in *Electronic and Atomic Collisions, Invited Papers of the XV International Conference on the Physics of Electronic and Atomic Collisions, Brighton, United Kingdom, 1987,* edited by H. B. Gilbody *et al.* (North-Holland, Amsterdam, 1988), p. 655.

[12]R. C. Isler and R. E. Olson, Phys. Rev. A **37**, 3399 (1988).

[13]R. E. Olson and A. Salop, Phys. Rev. A **16**, 531 (1977).

[14]B. C. Stratton *et al.*, Nucl. Fusion **30**, 675 (1990).

[15]S. D. Scott *et al.*, Phys. Rev. Lett. **64**, 531 (1990).

[16]B. C. Stratton *et al.*, Nucl. Fusion (to be published).

[17]K. W. Gentle, Phys. Fluids **31**, 1105 (1988).

[18]D. W. Ross *et al.*, Fusion Research Center, The University of Texas at Austin, Fusion Research Report No. FRCR 295, 1987 (unpublished).